Running title: Hydrostatic pressure hinders oil degradation

Reduced TCA cycle rates at high hydrostatic pressure hinder hydrocarbon degradation and obligate oil degraders in natural, deep-sea microbial communities

Alberto Scoma[1,2,3*], Robert Heyer[4], Ridwan Rifai[1], Christian Dandyk[4], Ian Marshall[2], Frederiek-Maarten Kerckhof[1], Angeliki Marietou[2], Henricus T.S. Boshker[5,6], Filip J. R. Meysman[5,6,7], Kirsten G. Malmos[8], Thomas Vosegaard[8], Pieter Vermeir[9], Ibrahim M. Banat[10], Dirk Benndorf[4,11] and Nico Boon[1]

1 Center for Microbial Ecology and Technology (CMET), Gent University, Coupure Links 653, B 9000 Gent, Belgium

2 Department of Bioscience, Microbiology Section, Aarhus University, Ny Munkegade 116, 8000 Aarhus C, Denmark

3 Biological and Chemical Engineering, Aarhus University, Hangøvej 2, 8200 Aarhus N, Denmark

4 Otto von Guericke University of Magdeburg, Bioprocess Engineering, Universitätsplatz 2 G25, 39106 Magdeburg, Germany

5 Department of Biotechnology, Delft University of Technology, Van der Maasweg 9, 2629 HZ Delft, The Netherlands

6 Department of Biology, University of Antwerp, Universiteitsplein 1, BE- 2610 Wilrijk (Antwerp), Belgium

7 Department of Analytical, Environmental and Geochemistry (AMGC), Vrije Univeriteit Brussel (VUB), Pleinlaan 2, 1050, Brussel, Belgium

8 iNANO, Department of Chemistry, Aarhus University, Gustav Wieds vej 14, 8000 Aarhus C, Denmark

9 Laboratory for Chemical Analyses (LCA), Department of Green Chemistry and Technology, Gent University, Valentin Vaerwyckweg 1, 9000 Ghent, Belgium

10 School of Biomedical Sciences, University of Ulster, Coleraine, N. Ireland, UK

11 Max Planck Institute for Dynamics of Complex Technical Systems, Bioprocess Engineering, Sandtorstraße 1, 39106 Magdeburg, Germany

***Corresponding author**:

Alberto Scoma

Department of Biological and Chemical Engineering,

Aarhus University, Hangøvej 2, 8200, Aarhus N, Denmark;

email: as@eng.au.dk; phone: +45 8715 6553

Abstract

Petroleum hydrocarbons reach the deep-sea following natural and anthropogenic factors. The process by which they enter deep-sea microbial food webs and impact the biogeochemical cycling of carbon and other elements is unclear. Hydrostatic pressure (HP) is a distinctive parameter of the deep sea, although rarely investigated. Whether HP alone affects the assembly and activity of oil-degrading communities remains to be resolved. Here we have demonstrated that hydrocarbon degradation in deep-sea microbial communities is lower at native HP (10 MPa, about 1 000 m below sea surface level) than at ambient pressure. In long-term enrichments, increased HP selectively inhibited obligate hydrocarbon-degraders and downregulated the expression of beta-oxidation-related proteins (*i.e.*, the main hydrocarbon-degradation pathway) resulting in low cell growth and CO_2 production. Short-term experiments with HP-adapted synthetic communities confirmed this data, revealing a HP-dependent accumulation of citrate and dihydroxyacetone. Citrate accumulation suggests rates of aerobic oxidation of fatty acids in the TCA cycle were reduced. Dihydroxyacetone is connected to citrate through glycerol metabolism and glycolysis, both upregulated with increased HP. High degradation rates by obligate hydrocarbon-degraders may thus be unfavourable at increased HP, explaining their selective suppression. Through lab-scale cultivation, the present study is the first to highlight a link between impaired cell metabolism and microbial community assembly in hydrocarbon degradation at high HP. Overall, this data indicates that hydrocarbons fate differs substantially in surface waters as compared to deep-sea environments, with *in situ* low temperature and limited nutrients availability expected to further prolong hydrocarbons persistence at deep sea.

Introduction

Every year more than 1 000 million liters of petroleum hydrocarbons enter the sea via natural seeps or anthropogenic activities [1]. Many microorganisms use hydrocarbons as a carbon and energy source [2], with metabolism affected by the chemical nature of the hydrocarbon, electron acceptor availability and temperature [3]. Hydrostatic pressure (HP) has been a largely neglected factor so far, in spite of being a distinctive geophysical parameter of deep-sea environments [4]. At increasing depths, the greater amount of mass in the water column exerts a downward force from the sea surface which is equal to about 1 MPa every 100 m (thus, HP is about 10 MPa at 1 000 m below sea surface level [bsl]). Microbial hydrocarbon degradation at natural seeps located up to 3 500 m bsl generates sufficient biomass to feed invertebrate communities [5]. In hot, anaerobic and nutrient-limited (*e.g.*, phosphate, sulphate) deep subsurface oil reservoirs, microbial hydrocarbon degradation can proceed on a geological timescale at the oil-water interface [6]. The consistent observation of microbial oil consumption in different deep-sea ecosystems suggests that this is a common process at increased HP.

Until recently, the main anthropogenic contribution to deep-sea oil contamination was linked to seepage from shipwrecks. There are about 9 000 potentially polluting wrecks laying on seafloors worldwide up to 6 000 m bsl, holding 3 000 to 23 000 million liters of oil [7, 8]. A more accurate assessment of the pathways of spilled-oil in the deep sea was carried out after the Deepwater Horizon (DWH) oil well blowout (Gulf of Mexico, April 2010). The DWH spill was the largest marine oil spill in history and the first to originate underwater (at 1 500 m bsl, ≈15 MPa) [9]. Research on microbial community composition and gene expression in deep-sea DWH samples indicated a response to petroleum hydrocarbons [10–12]. However, DWH deep-sea studies generally compared contaminated and uncontaminated samples from equivalent HPs. Environmental investigations comparing samples at different HPs along the

83 water column cannot avoid temperature gradients, which complicates results interpretation.
84 Microbial degradation represents the ultimate step for the clean-up of oil-contaminated
85 environments, particularly for the poorly accessible deep-sea areas. The process by which
86 petroleum hydrocarbons enter the deep-sea microbial food web and impact the carbon budget
87 and other biogeochemical cycles remains unresolved. This knowledge gap hampers the
88 development of bioremediation technologies to combat deep-sea spills. In particular, it is
89 unclear whether HP alone affects the assembly of oil-degrading microbial communities and
90 their metabolism.
91 In the present study, laboratory-scale cultivation was applied to selectively discriminate the
92 role of the sole HP in shaping the physiology and ecology of microbial hydrocarbon
93 degradation. Hydrocarbon-free, high HP-adapted surficial microbial communities in marine
94 sediments collected from 1 000 m bsl (≈10 MPa) were supplied with long-chain
95 hydrocarbons as sole carbon source. Long-chain hydrocarbons were selected because they
96 have a greater chance of reaching deep-sea environments (*e.g.*, following offshore *in situ*
97 burning, [13,14]), where they persist longer than short-chain aliphatics [15]. Following
98 enrichments in the pressure range 0.1 to 30 MPa, isolation was conducted to retrieve high
99 HP-adapted microorganisms, which were tested further in synthetic communities.
100
101 **Materials and Methods**
102 *Sample collection*
103 Sediment cores were collected at the West Iberian Margin (June 2-10, 2014, onboard the R/V
104 Belgica) using a multicorer at 960 m bsl for C_{20} incubations (latitude 37°49'579; longitude
105 09°27'497), and at 955 m bsl for C_{30} incubations (latitude 37°58'849; longitude 09°23'353).
106 The upper 2 cm of the sediment cores were used for experiments. Samples were kept at 4°C
107 and 10 MPa (*in situ* HP) using high HP reactors (HHPRs) until reaching the lab (17 days).

Microbial analyses

HHPRs. High HP incubations were conducted in stainless steel ISI 316 reactors (208 mL, maximum HP 60 MPa) (Nantong Feiyu Oil Science and Technology Exploitation, China). HP was delivered through a manual pump.

Microbial enrichments at different HP. The experimental set up is described in Fig. 1. Sediments were diluted 20% (w:v) with ONR7a medium [16], pH 7.5±0.1. The *n*-alkane eicosane (C_{20}) and triacontane (C_{30}) (Sigma-Aldrich, Belgium) were supplied as sole carbon source 0.1% (w:v). The liquid phase was 200 mL, with 8 mL of gas phase. O_2 was provided by injecting 2.5 MPa of air, subsequently increasing HP to 10 or 20 MPa by adding sterile medium. Two control reactors at ambient pressure (0.1 MPa) were set using different initial O_2 supply. For high O_2 levels, a Schott bottle was used (200 mL liquid phase, 950 mL of gas phase). For microaerophilic controls a HHPR was used (100 mL of liquid phase; 108 mL of gas phase). O_2 supply in microaerophilic controls was thus 10 to 2-fold lower as compared to high O_2 controls and HHPR, respectively. Two negative controls were also prepared (marine sediment and no added carbon; and sterile ONR7a with either C_{20} or C_{30} but no sediment). These control reactors were tested at 0.1 MPa. Before any re-inoculation, reactors were washed with ethanol 70% (v:v, Sigma Aldrich) and rinsed five times with autoclaved, milli-Q water. Media were autoclaved before use, but re-inoculation and incubation were not carried out aseptically. Reactors were incubated statically for 10 days at 20°C. Afterwards, pressure was gently released to ambient levels, the culture diluted ten-fold in fresh ONR7a medium and incubated again (nine consecutive incubations for a final enrichment of three months).

Isolation procedure and biomass characterization. Besides HHPRs operated at 10 and 20 MPa, with either hydrocarbon consortia enriched at 20 MPa were used as inoculum for new HHPRs operated at 30 MPa. All reactors were used for biomass characterization (*i.e.*, PLFAs

and amino acids). Isolation was attempted with HHPRs supplied with C_{20} at 10 and 20 MPa (Fig. 1) first at high HP and subsequently by plating (details provided in Supplementary Information).

Synthetic community experiments. Multispecies colonies from -80°C glycerol stocks (20%, v:v) were thawed and cultivated axenically on either acetate or C_{20} in ONR7a medium using 150 mL glass Schott bottles (50 mL liquid phase), under aerobic, static conditions at 20°C for 14 days. Two high HP-adapted synthetic communities were thus prepared: one grown on acetate and one on C_{20}. Synthetic communities had equal carbon content (*i.e.*, 0.8495 gC L^{-1} with either acetic acid or C_{20}) and initial cell number (2 x10^6 cells mL^{-1}) and were incubated in triplicate at 0.1 or 10 MPa in glass Schott bottles or HHRPs, under the same conditions as for enrichments.

Bacterial counts. Cell concentrations were assessed by flow cytometry with SYBR green I staining [17]. Cells were diluted 1:10^3 and 1:10^4 with autoclaved, filtered ONR7a medium (0.22 µm, Sartorius, Belgium), and fractioned according to their size using glass microfibers filters of 1.5 and 25 µm (Sartorius), with the latter used for total cell number.

Molecular Analyses

DNA extraction. Samples (2 mL) were centrifuged in a FastPrep tube (5 min, 13000 rpm). Then, pellets were supplied with 200 mg glass beads (0.11 mm, Sartorius) and 1 mL lysis buffer (100 mM Tris, 100 mM EDTA, 100 mM NaCl, 1% polyvinylpyrrolidone [PVP40], 2% sodium dodecyl sulphate [SDS]; pH 8). Tubes were placed in a FastPrep device (MP Biomedicals, USA) (16000 rpm, 40 s, 2 runs), centrifuged (10 min, maximum speed, 4°C), the DNA extracted with phenol-chloroform and precipitated with ice-cold isopropyl alcohol and 3 M sodium acetate (1 h, -20°C). Isopropyl alcohol was removed by centrifugation (30 min, max speed), DNA pellets dried and resuspended in TE buffer (10 mM Tris, 1 mM

158 EDTA) and stored at -20°C. DNA sample quality was assessed using 1% (w:v) agarose (Life
159 technologies™, Spain) gel-electrophoresis, and quantified by a fluorescence assay
160 (QuantiFluor® dsDNA kit; Promega, USA) using a Glomax®-Multi+ system (Promega).
161 Samples were normalized to 1 ng μL^{-1} DNA and sent to LGC Genomics (Germany) for
162 library preparation and sequencing using the Illumina Miseq platform (details provided in
163 Supplementary Information).
164 Metagenome sequencing. DNA extracted from multispecies colonies was used for
165 metagenome sequencing on an Illumina MiSeq platform. 16S rRNA genes were extracted
166 from assembled metagenomic contigs, with contig coverage calculated to estimate relative
167 abundance of each strain in each enrichment (details provided in Supplementary
168 Information).
169
170 *Metaproteome analysis*
171 Culture samples (100 mL) were centrifuged, pellets dissolved in 400 µL 50 mM Tris/HCl
172 (pH 6.8) and protein extracted with liquid phenol [18]. After protein quantification with
173 amido black assay, 7 µg of proteins from the enrichments and 25 µg from the synthetic
174 communities were loaded into a 12% SDS-PAGE. For enrichments, the SDS-PAGE was
175 conducted after proteins entered approximately 5 mm into the separation gel, while for
176 synthetic communities each lane was cut afterwards in ten equal fractions for LC-MS/MS
177 measurements. The complete protein fraction was digested with trypsin, and peptides were
178 measured by LC-MS/MS using an Elite Hybrid Ion Trap Orbitrap MS with a 120 min
179 gradient. For protein identification, a database search with Mascot [19] was performed, using
180 a false discovery rate of 1% (details provided in Supplementary Information). All MS results
181 were submitted to PRIDE [20], accession number PXD004328.
182

Statistical analysis

Bars in the graphs indicate a 95% confidence interval (95% CI) calculated using a Student *t*-test with a two-sided distribution. Statistical significance was assessed using a nonparametric test (Mann-Whitney test) which considered a two-sided distribution with 95% CI. Differential abundance analysis of 16S rRNA amplicon OTUs was conducted using ALDEx2 (v.1.10.0) [21, 22] on OTUs combined into families. High HP samples (10 or 20 MPa) were compared to ambient pressure controls (aerobic and microaerophilic). Families where the Wilcoxon signed-rank test yielded $p < 0.05$ were considered significantly differentially abundant in between the two conditions.

Chemical analyses

Dissolved O_2 was measured with a probe by Hach (Belgium). pH was determined with a probe by Metrohm (Belgium). Phosphate and sulphate were quantified with a Compact Ion Chromatograph (Metrohm, Switzerland) equipped with a conductivity detector. Dissolved inorganic carbon was determined by gas chromatography (SRI 310C, USA) after adding 10% H_3PO_4 (Sigma-Aldrich).

Intracellular metabolites Samples were prepared with minor modifications according to [23]. NMR spectra were obtained on Bruker spectrometers operating at 500 and 700 MHz (^{1}H), processed using MestReNova (v.11.0.4, Mestrelab Reserch), and analyzed by pcaMethods package [24] using R (v.3.4.4) (details provided in Supplementary Information).

Results

High HP selects for small-sized cell cultures with high nutrient uptake but low biomass yield and hydrocarbon-degradation capacity

Hydrocarbon-free surficial marine sediment collected at 1 000 m bsl (≈10 MPa) was incubated at increased HP (10 or 20 MPa) under aerobic conditions, using control cultures at atmospheric pressure (0.1 MPa) under aerobic and microaerophilic conditions. Cultures were supplied with either C_{20} or C_{30} as sole carbon source and grown for 3 months under repeated batch conditions (9 incubations of 10 days each, 10% dilution; experimental set up in Fig. 1). To assess microbial oil degradation capacity, the pH of test reactors was compared with two negative controls, one without added carbon and another without marine sediment (Fig. 2). Provided that either C_{20} or C_{30} were supplied as sole carbon source, decreased pH values indicated high hydrocarbon degradation activity, as CO_2 ionization in water generates HCO_3^- + H^+. All test reactors showed a lower pH with respect to negative controls throughout the whole enrichment (p <0.05, Fig. 2). After three repeated inoculations (*i.e.*, 30 days) the marine sediment was completely washed out from all reactors, thus the potential contribution of microbes attached to the sediment was removed. In controls with no C_{20} or C_{30}, this resulted in negligible cell counts (as assessed by flow cytometry; these controls were stopped after 50 days). HP reactors showed a lower acidification capacity compared to both control cultures at 0.1 MPa (Fig. 2). This was particularly evident in enrichments with C_{30}, as after 70 days cultures at increased HP showed a loss of acidification capacity and could not decrease the pH below about 7.15 at any new batch incubation (Fig. 2). This was not reflected in any other physiological measurement, as enriching cultures were comparable between 30 and 90 days (Fig. 3). Cultures at high HP generally had a lower cell number as compared to ambient controls with either carbon source (Fig. 3A,B), and were characterized by an increasingly smaller size (as assessed by flow cytometry on 1.5-µm-filtered samples, Fig. 3C,D). Small-sized cells were not merely due to a physical constraint (if any) imposed by high HP, as cell counts were conducted 1-2 h after decompression. Irrespective of the HP

231 applied, cultures supplied with C_{20} had lower pH values than those at C_{30}, while the latter had
232 a higher cell number.
233 At ambient conditions, C_{20} and C_{30} are solid and solubilize in water at less than 2 μg L^{-1} [25].
234 Quantitative hydrocarbon degradation measurements would thus require extraction with
235 solvents of the entire culture, preventing further culturing. However, of the 72 reactors tested
236 through the enrichments, hydrocarbons were found in the water phase only in one case (20
237 MPa, 9th incubation, C_{20}), indicating that hydrocarbon solubilisation was likely followed by
238 rapid bacterial consumption.
239 HP did not significantly alter O_2 respiration per cell with either carbon source (p >0.05, Fig.
240 3E,F). Nonetheless, high HP stimulated SO_4^{2-} reduction per cell, which was higher than
241 aerobic controls and generally comparable to microaerophilic controls (p <0.05; Fig. 3G,H).
242 This must take into account that the total amount of O_2 respired by the cells in high HP
243 reactors was higher than in microaerophilic controls (p <0.05, Fig. S1A,D). Finally, with
244 either carbon source high HP enhanced PO_4^{3-} consumption per cell as compared to both
245 controls at ambient pressure (p <0.05; Fig. 3I,J).
246
247 *High HP inhibits specialized, hydrocarbonoclastic bacteria and selects for generic,*
248 *nonspecific oil-degraders*
249 Long-chain-hydrocarbon supply to pristine sediments resulted in a remarkable microbial
250 succession (Fig. 4A). A shared response to increased HP with either hydrocarbon was the
251 significant abundance of *Desulfuromonadaceae* as opposed to *Oceanospirillaceae* in ambient
252 controls (p <0.05, Table S1A,B; Fig. 4A). At high HP, supply of C_{20} also significantly
253 enriched *Halomonadaceae*, *Pseudoalteromonadaceae* and *Shewanellaceae*, with
254 *Vibrionaceae* significantly more enriched only with C_{30} (p <0.05, Table S1A,B). A time
255 course of the most enriched genera is presented in Table S2, S3 and Fig. S2. Some of the so-

called obligate hydrocarbonoclastic bacteria (OHCB), a group of specialized marine microorganisms growing almost exclusively on oil [26], were present in our enrichments (*e.g.*, *Thalassolituus* and *Alcanivorax*). While predominating in both controls at ambient pressure, OHCB were almost totally suppressed by high HP (Fig. 4B).

High HP downregulates β-*oxidation and increases housekeeping proteins*

High HP in enriched consortia (90 days) shaped cell metabolism as described by metaproteome analyses, particularly concerning house-keeping functions. Expression of proteins related to biological functions (UniProtKB keyword) such as ATP synthesis, ion and proton transport were upregulated with high HP as compared to ambient controls, while transcription was downregulated (p <0.05, Fig. 5; Table S4). The increased importance of ions and protons transport may relate to the acidification following hydrocarbon oxidation, as cells at high HP might experience lower pH values due to increased CO_2 solubility (16% equilibrium pressure increase every 10 MPa [27]) and facilitated ionization as compared to atmospheric pressure [28]. Among the low abundance proteins, high HP negatively impacted lipid degradation, fatty acid and lipid metabolism (p <0.05, Fig. 5; Table S4). In particular, metaproteins related to fatty acids β-oxidation (EC: 4.2.1.17; 5.1.2.3; 5.3.3.8; 1.1.1.35; 2.3.1.9; 1.3.99.-) were remarkably downregulated at high HP with either carbon source (p <0.025; log2 fold change [f.c.] -1.53 to -3.80; Table S5A,B). Mapped metaproteins comprised enzymes required for detoxification of radical O_2 species, suggestive of an active hydrocarbon oxidation at high HP and aerobic controls at ambient pressure (Table S5). However, O_2 stress at high HP was equal or lower than in aerobic controls at ambient pressure (Table S5A,B), indicating that the enhanced dissolved O_2 levels imposed by a HP increase (14% equilibrium pressure increase every 10 MPa for O_2 [27]) did not turn into a stress factor for the cultures. Nonetheless, several proteins for sulphite (SO_3^{2-}) reduction in

high HP enrichments confirmed that O_2 respiration was followed by anaerobiosis and SO_4^{2-} reduction with either carbon source (Fig. 3G,H). Finally, although proteins for alkane degradation were identified, the alkane 1-monooxygenase (EC: 1.14.15.3) responsible for terminal oxidation [29] was only detected with C_{30} in aerobic controls at ambient pressure (Table S6).

High HP increases short and branched-chain PLFAs

With either hydrocarbon, cultures at 20 MPa were used to inoculate reactors at 30 MPa (Fig. 1), and HP impact on PLFA and amino acid profiles was investigated. High HP increased the relative abundance of shorter PLFAs, in particular C15 and C16 (p <0.01, log2 f.c. 2.9 to 3.3; Fig. S3A,C). The relative content of iso-, anteiso- and in general total branched-chain PLFAs was remarkably higher at high HP as compared to both controls at ambient pressure, contrary to cyclopropane PLFAs (p <0.015, log2 f.c. -0.9 to -3.1; Fig. S3B,D). High HP-enriched consortia accumulated *i*-C15:0, *ai*-C15:0, *i*-C16:0, C16:1ω7t, *i*-C17:1ω7c and two undetermined PLFAs (p <0.05; Fig. S4A,B), while carrying less C18 monounsaturated PLFAs, especially C18:1ω9c (Fig S4A,B). Amino acid profiles were not affected by HP except in consortia supplied with C_{30} ≥20 MPa (Table S7).

Isolation from HP-enriched consortia yields multispecies colonies of generic, nonspecific oil-degrading bacteria

Isolation from enriched consortia at 10 and 20 MPa was attempted with C_{20} under aerobic conditions. Following dilution (up to 10^{-9}), cultures were cultivated at their respective HP, then streaked on agar at ambient pressure. Colonies were generally no more than five per plate, possibly due to the reduced access to the solid C_{20} used as sole carbon source, and less than 1 mm in diameter. Each colony yielded metagenomes with two to five unique 16S rRNA

306 gene sequences (Table S8), and thus represented a reduced complexity of the source
307 community rather than a pure isolate. The assembly of such multispecies colonies did not
308 differ when derived from either 10 or 20 MPa (Table S8). However, when considered
309 together the 11 multispecies colonies retrieved from high HP-enriched consortia were formed
310 by a core community of four frequently recurrent genera (*Thalassospira*, *Vibrio*, *Halomonas*
311 and *Pseudoalteromonas*) which were among the most abundant at high HP (Table S2C,D) or
312 whose family was significantly enriched at high HP (*Halomonadaceae* and
313 *Pseudoalteromonadaceae* with C_{20}, Table S1). None of these recurring genera was a
314 specialized OHCB. On the contrary, the less frequent genera (*e.g.*, *Thalassolituus*,
315 *Pseudomonas*, *Microbacterium*) were neither abundant at high HP (Table S4C,D) nor
316 belonged to families associated to high HP (Table S1). The reason for yielding multispecies
317 colonies in place of individual species is unclear. The absence of *Deltaproteobacteria* is
318 considered a consequence of adopting aerobic conditions for isolation.
319
320 *High HP-adapted synthetic communities confirm a shift from OHCB to generic, nonspecific*
321 *oil-degraders with reduced hydrocarbon-degradation capacity*
322 Multispecies colonies originated from the C_{20} consortia enriched at 10 and 20 MPa were used
323 as inoculum to assemble a high HP-adapted synthetic community (HHP-SC), which was
324 tested at 0.1 and 10 MPa using as sole carbon source either C_{20} or acetate as control (Fig. 1).
325 HHP-SCs performance in terms of acidification capacity and growth was comparable with
326 that of enriched consortia selected under equivalent increased HPs (*i.e.*, 10 MPa; $p > 0.05$,
327 Fig. 6A,B). Thus, HHP-SCs reliably reproduced the hydrocarbon degradation capacity of HP
328 enrichments even in the absence of isolated *Deltaproteobacteria*. Moreover, when such HHP-
329 SCs were tested at ambient pressure their performance was lower as compared to consortia

enriched in long-term experiments at 0.1 MPa (p <0.05, Fig. 6A,B), which were largely dominated by the OHCB *Thalassolituus* (Fig. S2).

Increased HP reduced cell growth of HHP-SCs irrespective of the supplied carbon source (Fig. 6C), resulting in low total CO_2 productions (Fig. S5) although HHP-SCs microbial community composition was not dramatically altered by the different conditions applied. Despite being tested under non-axenic conditions, HHP-SCs were represented by only eight main OTUs (99.0 to 99.4% of the total 16S rRNA sequences, Table 1), all originally present in the multispecies colonies used as inoculum (Fig. S6). In particular, HHP-SCs were constituted by a core community of four OTUs which were the most represented, especially in the test condition (*i.e.*, 10 MPa, C_{20}; 96.4%, Table 1). This core community was constituted by the four generic, nonspecific oil-degrading genera *Vibrio*, *Thalassospira*, *Halomonas* and *Pseudoalteromonas* found to be frequently recurrent in multispecies colonies (Table S8). The OHCB *T. oleiovorans* (OTU00005, SSU_type8, Fig. S6) grew at ambient pressure in the presence of C_{20} but was inhibited at 10 MPa (16S rRNA abundance from 10.7 to 1.5%, log2 f.c. -2.8; Table 1), as occurred in enrichments (Fig. 4B).

High HP leads to intracellular citrate and dihydroxyacetone accumulation

Cell metabolism in HHP-SCs was analysed. The full metaproteomes related to alkane activation and *β*-oxidation could be reconstructed, with the exception of the alkane 1-monooxygenase (EC: 1.14.15.3) responsible for terminal oxidation [29] (Fig. S7), as for enrichments (Table S6). A deeper analysis of the alkane-activation mechanism is proposed in the Supplementary Information. Incubation of HHP-SCs under ambient pressure did not restore high expression levels of *β*-oxidation-related proteins as compared to high HP (Table S9), nor did it with lipid and fatty acid metabolism, or lipid degradation-related metaproteins (p >0.05; Table S10). However, high HP upregulated glycerol metabolism (log2 f.c. +0.76

355 [C_{20}] and +0.67 [acetate], Table S10). The possibility that glycerol may have been used to
356 produce biosurfactants [30], a group of glycolipids, phospholipids and lipoproteins enhancing
357 the apparent solubility of oil in water, was not supported by surface tension and
358 emulsification property analysis (Table S11). However, the entire metaproteome connecting
359 glycerol metabolism to the tricarboxylic acid cycle (TCA) could be reconstructed (Fig. 7A).
360 Two key intermediates of these pathways interconnected by few enzymatic reactions, namely
361 citrate and dihydroxyacetone, were significantly accumulated in cells at high HP (Fig. 7B), in
362 the frame of a general HP-dependent rearrangement of water and lipid-soluble intracellular
363 metabolites (p <0.05; Fig. 7C, Fig. S8-10).
364
365 **Discussion**
366 The use of increased HP in laboratory-scale experiments is an emerging approach to
367 investigate deep-sea oil degradation [31-38]. While the use of reactors may reduce microbial
368 biodiversity to cultivable species, in the case of HP it allows to simulate a poorly accessible
369 environment such as the deep sea. Existing literature indicates that enhanced HP affects
370 bacterial hydrocarbon consumption, however it does not explain the relationship between HP,
371 microbial community assembly, and hydrocarbon degradation capacity. Whether oil-
372 degradation pathways differ between surface and deep sea remains unclear. In the present
373 study, we used pristine marine sediment microbial communities natively adapted to 10 MPa
374 (*i.e.*, 1 000 m bsl) to decipher the sole effect of HP on microbial hydrocarbon metabolism
375 independent of other parameters that may differ along the water column. HPs up to 30 MPa
376 (3 000 m bsl) were tested on either 1) enriched consortia or 2) synthetic communities adapted
377 to high HP (HHP-SCs). The first approach tested the impact of HP on the long-term selection
378 of different microbial community members, while the second focused on the short-term
379 impact of HP on the metabolism of comparable communities already adapted to high HP.

Long-term selection of high HP in enriching oil-degrading consortia

The supply of long-chain hydrocarbons (either C_{20} or C_{30}) to pristine sediments resulted in a HP-dependent restructuring of microbial communities (Fig. 4A). The OHCB *Thalassolituus* and *Alcanivorax* that largely predominated in ambient pressure controls (irrespective of O_2 availability) were suppressed by a HP increase to only 10 MPa (Fig. 4B). As HP application enhances gas solubilisation [27], cells ≥10 MPa might have experienced higher dissolved O_2 levels, which potentially influenced hydrocarbon metabolism and microbial community assembly. However, O_2 respiration per cell was not impacted by high HP (Fig. 3E,F) and proteins related to O_2 stress were equally expressed in aerobic controls and high HP-enriched consortia (Table S5).

High HP increasingly selected for small-sized (Fig. 3C,D), slow-growing (Fig. 3A,B) cells. Although not impacting cell respiration, at high HP anaerobiosis was established during each 10-day incubation, prompted SO_4^{2-} reduction (Fig. 3G,H; Table S5) and stimulated the enrichment of unique *Deltaproteobacteria* (*i.e.*, *Desulfuromonadaceae*; Table S1, S2, S3; Fig. S2) as compared to microaerophilic controls at ambient pressure. The observed shift in PLFA profiles reflected these changes in microbial community assembly. In fact, the PLFA composition at ambient pressure resembled that of obligate oil-degraders [39-41], while the increase in uneven branched-chain PLFAs under high HP (particularly i17:1ω7c) probably mirrored the increase in *Deltaproteobacteria* [42-44]. In particular, high HP selected for consortia remarkably enriched in branched-chain PLFAs (Fig. S3), a typical response of HP-tolerant microbes [45].

High HP-enriched consortia were characterized by low expression levels of *β*-oxidation-related proteins (Fig. 5; Table S5), consistent with previous findings by members of the present group on transcript levels of two axenic *Alcanivorax* species inhibited by 10 MPa

405 while supplied with *n*-dodecane [36, 37]. *β*-oxidation represents the main metabolic pathway
406 for hydrocarbon degradation following their activation [2]. A reduced protein expression
407 level does not imply *per se* that a pathway is not operating, rather that it plays a less relevant
408 role under the tested conditions. When compared to ambient controls, high HP-enriched
409 consortia were featured by increased expression levels of housekeeping proteins, particularly
410 basic cellular functions such as ATP synthesis and ion transport including hydrogen (Fig. 5,
411 Table S4). pH homeostasis is based on a H^+-ATPase and is influenced by CO_2 production
412 [28], and hydration and ionization of CO_2 is facilitated at increased HP as it entails negative
413 volume changes [28]. Thus, maintenance of pH homeostasis in acidifying cultures oxidizing
414 hydrocarbons may represent a critical function at increased HP. In bacteria, high HP
415 increases membrane permeability and inactivates pH-maintaining enzymes [46-48].
416 Permeability to ions impairs proton-driven forces used by several pumps (*e.g.*, Na/K ATPase,
417 [49]), a correlation being observed between ion pump activity and HP [50]. A similar
418 molecular response (*i.e.*, impacted ATP synthesis and expression of Na^+-translocating
419 reductases) was reported in the transcriptomic studies on the two axenic *Alcanivorax* species
420 supplied with *n*-dodecane and inhibited at 10 MPa [36, 37]. Sustained hydrocarbons
421 oxidation at increased HP may thus entail increased cell maintenance, rendering high *β*-
422 oxidation levels less favourable.
423
424 *Short-term effect of high HP on hydrocarbon metabolism in synthetic communities*
425 Isolation from high HP-enriched consortia yielded multispecies colonies where a core
426 community of high HP-adapted genera was associated with satellite microorganisms not
427 related to HP. Among the latter, the OHCB *T. oleiovorans* was detected (Table S8). When
428 tested in HHP-SCs with C_{20}, *T. oleiovorans* could grow at ambient pressure but was inhibited
429 by a HP increase to only 10 MPa (Table 1). This was consistent with the enrichment findings

(Fig. 4B) and extends to *Thalassolituus* the so-called "*Alcanivorax* paradox" hypothesis proposed by some of the present authors [51]. This notes that in both field and lab-scale experiments so far OHCB appear to be affected by increased HPs [4]. Variation in temperature, salinity, electron acceptor availability, hydrocarbons and possibly pH in concomitance with increased HP is expected to refine this observation. For instance, the increased relative abundance of the OHCB genus *Cycloclasticus* [26] was correlated with the enrichment of aromatic hydrocarbons in underwater oil plumes during the DWH [52], however experimental evidence with lab-scale HP tests is missing. Recent findings report that a close relative of the OHCB, psychrophilic *Oleispira antarctica* RB-8 could grow in DWH deep-seawater samples in short-term (32 days), lab-scale tests when high HP was applied in combination with low temperature (0.1 to 30 MPa, 4°C) using Macondo oil [53]. *O. antartica* predominated at all HPs, its selective advantage likely being dependent on the low temperature concomitantly applied (it was isolated from Antarctic coastal water [54]). Interestingly, its relative abundance slightly decreased with increasing HP (81 to 65%, 0.1 to 30 MPa). No other OHCB was detected, contrary to several generic, nonspecific oil-degraders, many of which consistent with the present study (*e.g.*, *Vibrio*, *Photobacterium* and *Marinifilum*; Table S2, S3; [53]).

Another prominent effect of high HP in combination with low temperature was to reduce growth [53], as reported earlier [31]. In the present study, this occurred only by increasing HP (Fig. 3A,B; Fig. 6C). In particular, comparable HHP-SCs (Table 1) underwent a 5-fold decrease in growth yields when increasing HP to only 10 MPa. The latter was consistent with the intracellular accumulation of citrate and dihydroxyacetone (Fig. 7B), two metabolic intermediates linked by few reactions whose enzymes were detected by metaproteomics (Fig. 7A). Citrate is the key intermediate of the TCA cycle, an aerobic process involved in the final steps of fatty acids (and carbohydrates) oxidation generating NADH for use *e.g.* in ATP

455 synthesis, a biological function upregulated at increased HP in long-term enrichments (Fig.
456 5). Citrate HP-dependent accumulation suggests a reduction of TCA cycle rates, apparently
457 related with the accumulation of dihydroxyacetone. The significant upregulation of the
458 biological functions glycerol metabolism and glycolysis interconnecting these two metabolic
459 intermediates supports this hypothesis (Tab. S10). The possibility that dihydroxyacetone
460 represents a novel piezolyte, *i.e.*, a solute whose biosynthesis is triggered by HP increases
461 [55], cannot be discarded. The reason for reduced TCA cycle rates under increased HP is
462 unclear. Aconitase and isocitrate dehydrogenase, the enzymes using citrate and its product in
463 the TCA cycle, can be completely inhibited after only 15 min at HPs 5-15 times greater than
464 what applied in the present study [56]. Whether their catalytic activity is partially inhibited at
465 10 MPa needs further investigation.
466 In conclusion, the present dataset reports the first comprehensive overview describing how
467 HP shapes the physiology and ecology of microbial hydrocarbons degradation. A reduced
468 capacity to conduct the final steps of fatty acids oxidation (*i.e.*, TCA cycle) would decrease
469 *β*-oxidation levels, resulting in low cell growth and hydrocarbon mineralization. The selective
470 advantage of OHCB to sustain high hydrocarbon degradation rates would thus be prevented
471 at high HP, allowing generic, non-specific oil-degraders to thrive. In fact, reduced
472 hydrocarbon oxidation in high HP reactors occurred notwithstanding the availability of
473 electron acceptors, with enhanced HP requiring a higher expenditure for maintenance of cell
474 homeostasis (*e.g.*, ATP synthesis and ion transport), which involved cell membrane
475 composition (enriched in branched-chain PLFAs). The interplay between TCA cycle, ATP
476 synthesis, pH homeostasis and hydrocarbon oxidation at deep-sea HP should be investigated
477 further. This is particularly relevant to assess the fate of hydrocarbons entering the deep sea
478 following anthropogenic spills, where degradation of the overabundant hydrocarbon input is
479 further reduced by low temperature and lack of nutrients.

Acknowledgements

These findings were financially supported by the FP7-EU project Kill Spill (312139), the Geconcentreerde Onderzoeksactie, Ghent University (BOF15/GOA/006), the Danish Ministry of Higher Education and Science (AU-2010-612-181) and The Novonordisk Foundation (NNF16OC0021110). F.-M. Kerckhof was supported by the Inter-University Attraction Pole 'μ-manager' (BELSPO, P7/25). AS thanks Dr. Ann Vanreusel (Ghent University, Belgium) for her supervision during deep-sea sampling. Dr. Xiao Xiang and Yu Zhang (Shanghai Jiao Tong University, China) are acknowledged for their assistance with high-pressure reactors. A. Bastian (Otto von Guericke University of Magdeburg) and Katrine Bay Jensen (Aarhus University) are acknowledged for their technical assistance.

Conflict of Interest

The authors declare no conflict of interest

References

1. Maribus. World Ocean Review 3. 2014.
2. Rojo F. Degradation of alkanes by bacteria: Minireview. *Environ Microbiol* . 2009. , **11**: 2477–2490
3. Head IM, Jones DM, Röling WFM. Marine microorganisms make a meal of oil. *Nat Rev Microbiol* 2006; **4**: 173–182.
4. Scoma A, Yakimov MM, Boon N. Challenging oil bioremediation at deep-sea hydrostatic pressure. *Front Microbiol* 2016.

503 5. Jørgensen BB, Boetius A. Feast and famine — microbial life in the deep-sea bed. *Nat*
504 *Rev Microbiol* 2007; **5**: 770–781.

505 6. Head IM, Jones DM, Larter SR. Biological activity in the deep subsurface and the
506 origin of heavy oil. *Nature* 2003; **426**: 344–352.

507 7. NOAA. Oil spill case histories 1967-1991. 1992. Seattle, Washington.

508 8. Michel J, Gilbert T, Etkin DS. Potentially polluting wrecks in marine waters. *An Issue*
509 *Pap Prep 2005 Int Oil Spill Conf* 2005.

510 9. Federal Interagency Solutions Group. Oil Budget Calculator Science and Engineering
511 team 2010. Oil budget calculator technical documentation. 2010; 1–49.

512 10. Kimes NE, Callaghan A V., Suflita JM, Morris PJ. Microbial transformation of the
513 deepwater horizon oil spill-past, present, and future perspectives. *Front Microbiol* .
514 2014.

515 11. Joye SB, Teske AP, Kostka JE. Microbial dynamics following the macondo oil well
516 blowout across gulf of Mexico environments. *Bioscience* 2014.

517 12. King GM, Kostka JE, Hazen TC, Sobecky PA. Microbial Responses to the *Deepwater*
518 *Horizon* Oil Spill: From Coastal Wetlands to the Deep Sea. *Ann Rev Mar Sci* 2015.

519 13. Buist, I., Trudel, K., Morrison, J. & Aurand, D. Laboratory studies of the properties of in-
520 situ burn residues. *1997 International Oil Spill Conference* **1997**, 149-156,
521 doi:10.7901/2169-3358-1997-1-149 (1997).

522 14 Jézéquel, R., Simon, R. & Pirot, V. Development of a Burning Bench Dedicated to In
523 Situ Burning Study: Assessment of Oil Nature and Weathering Effect. *Proceedings of*
524 *the Thirty-seventh AMOP Technical Seminar on Environmental Contamination and*
525 *Response, Environment Canada, Ottawa, ON*, 555-566 (2014).

15 Bagby, S. C., Reddy, C. M., Aeppli, C., Fisher, G. B. & Valentine, D. L. Persistence and biodegradation of oil at the ocean floor following Deepwater Horizon. *Proc Natl Acad Sci U S A* **114**, E9-E18, doi:10.1073/pnas.1610110114 (2017).

16. Dyksterhouse SE, Gray JP, Herwig RP, Lara JC, Staley JT. Cycloclasticus pugetii gen. nov., sp. nov., an Aromatic Hydrocarbon-Degrading Bacterium from Marine Sediments. *Int J Syst Bacteriol* 1995; **45**: 116–123.

17. De Roy K, Clement L, Thas O, Wang Y, Boon N. Flow cytometry for fast microbial community fingerprinting. *Water Res* 2012; **46**: 907–919.

18. Heyer R, Kohrs F, Benndorf D, Rapp E, Kausmann R, Heiermann M, et al. Metaproteome analysis of the microbial communities in agricultural biogas plants. *N Biotechnol* 2013; **30**: 614–622.

19. Perkins DN, Pappin DJC, Creasy DM, Cottrell JS. Probability-based protein identification by searching sequence databases using mass spectrometry data. *Electrophoresis* 1999; **20**: 3551–3567.

20. Vizcaíno JA, Côté RG, Csordas A, Dianes JA, Fabregat A, Foster JM, et al. The Proteomics Identifications (PRIDE) database and associated tools: Status in 2013. *Nucleic Acids Res* 2013.

21. Fernandes AD, Macklaim JM, Linn TG, Reid G, Gloor GB. ANOVA-Like Differential Expression (ALDEx) Analysis for Mixed Population RNA-Seq. *PLoS One* 2013; **8**: e67019.

22. Fernandes AD, Reid JN, Macklaim JM, McMurrough TA, Edgell DR, Gloor GB. Unifying the analysis of high-throughput sequencing datasets: characterizing RNA-seq, 16S rRNA gene sequencing and selective growth experiments by compositional data analysis. *Microbiome* 2014; **2**: 15.

550 23. Tremaroli V, Workentine ML, Weljie AM, Vogel HJ, Ceri H, Viti C, et al.
551 Metabolomic investigation of the bacterial response to a metal challenge. *Appl Environ*
552 *Microbiol* 2009.

553 24. Stacklies W, Redestig H, Scholz M, Walther D, Selbig J. pcaMethods - A
554 bioconductor package providing PCA methods for incomplete data. *Bioinformatics*
555 2007.

556 25. MacKay D, Shiu WY. A critical review of Henry's law constants for chemicals of
557 environmental interest. *J Phys Chem*. 1981; **10**(4): 1175-1199

558 26. Yakimov MM, Timmis KN, Golyshin PN. Obligate oil-degrading marine bacteria.
559 *Curr Opin Biotechnol* 2007; **18**: 257–266

560 27. Enns T, Scholander PF, Bradstreet ED. Effect of hydrostatic pressure on gases
561 dissolved in water. *J Phys Chem* 1965.

562 28. Abe F, Horikoshi K. Analysis of intracellular pH in the yeast Saccharomyces
563 cerevisiae under elevated hydrostatic pressure: A study in baro- (piezo-) physiology.
564 *Extremophiles*, 1998.

565 29. Ji Y, Mao G, Wang Y, Bartlam M. Structural insights into diversity and n-alkane
566 biodegradation mechanisms of alkane hydroxylases. *Front Microbiol* 2013.

567 30. Dobler L, Vilela LF, Almeida R V., Neves BC. Rhamnolipids in perspective: Gene
568 regulatory pathways, metabolic engineering, production and technological forecasting.
569 *N Biotechnol*, 2016.

570 31. Schwarz JR, Walder JD, Colwell RR. Deep-sea bacteria: growth and utilization of n-
571 hexadecane at in situ temperature and pressure. *Can J Microbiol* 1975; **21**: 682–687.

572 32. Schwarz JR, Walder JD, Colwell RR. Deep-sea bacteria: growth and utilization of

573 hydrocarbons at ambient and in situ pressure. *Appl Microbiol* 1974; **28**: 982–986.

574 33. Grossi V, Yakimov MM, Ali B Al, Tapilatu Y, Cuny P, Goutx M, et al. Hydrostatic
575 pressure affects membrane and storage lipid compositions of the piezotolerant
576 hydrocarbon-degrading Marinobacter hydrocarbonoclasticus strain #5. *Environ*
577 *Microbiol* 2010; **12**: 2020–2033.

578 34. Schedler M, Hiessl R, Valladares Juárez AG, Gust G, Müller R. Effect of high
579 pressure on hydrocarbon-degrading bacteria. *AMB Express* 2014.

580 35. Fasca H, de Castilho LVA, de Castilho JFM, Pasqualino IP, Alvarez VM, de Azevedo
581 Jurelevicius D, et al. Response of marine bacteria to oil contamination and to high
582 pressure and low temperature deep sea conditions. *Microbiologyopen* 2018; **7**: e00550.

583 36. Scoma A, Barbato M, Borin S, Daffonchio D, Boon N. An impaired metabolic
584 response to hydrostatic pressure explains Alcanivorax borkumensis recorded
585 distribution in the deep marine water column. *Sci Rep* 2016; **6**: 31316.

586 37. Scoma A, Barbato M, Hernandez-Sanabria E, Mapelli F, Daffonchio D, Borin S, et al.
587 Microbial oil-degradation under mild hydrostatic pressure (10 MPa): which pathways
588 are impacted in piezosensitive hydrocarbonoclastic bacteria? *Sci Rep* 2016; **6**: 23526.

589 38. Scoma A, Boon N. Osmotic stress confers enhanced cell integrity to hydrostatic
590 pressure but impairs growth in Alcanivorax borkumensis SK2. *Front Microbiol* 2016.

591 39. Yakimov MM, Giuliano L, Denaro R, Crisafi E, Chernikova TN, Abraham WR, et al.
592 Thalassolituus oleivorans gen. nov., sp. nov., a novel marine bacterium that obligately
593 utilizes hydrocarbons. *Int J Syst Evol Microbiol* 2004.

594 40. Yakimov MM, Golyshin PN, Lang S, Moore ERB, Abraham W, Lunsdorf H, et al.
595 Alcanivorax borkurnensis gen. now, sp. nov., a New, Hydrocarbon-Degrading and
596 Surfactant-Producing Marine Bacterium. *Int J Syst Bacteriol* 1998; **48**: 339–348.

41. Liu C, Shao Z. Alcanivorax dieselolei sp. nov., a novel alkane-degrading bacterium isolated from sea water and deep-sea sediment. *Int J Syst Evol Microbiol* 2005.

42. Taylor J, Parkes RJ. The Cellular Fatty Acids of the Sulphate-reducing Bacteria, Desulfobacter sp., Desulfobulbus sp. and Desulfovibrio desulfuricans. *Microbiology* 1983.

43. Vainshtein M, Hippe H, Kroppenstedt RM. Cellular Fatty Acid Composition of Desulfovibrio Species and Its Use in Classification of Sulfate-reducing Bacteria. *Syst Appl Microbiol* 1992.

44. Kohring LL, Ringelberg DB, Devereux R, Stahl DA, Mittelman MW, White DC. Comparison of phylogenetic relationships based on phospholipid fatty acid profiles and ribosomal RNA sequence similarities among dissimilatory sulfate-reducing bacteria. *FEMS Microbiol Lett* 1994.

45. Wang F, Xiao X, Ou H-Y, Gai Y, Wang F. Role and Regulation of Fatty Acid Biosynthesis in the Response of Shewanella piezotolerans WP3 to Different Temperatures and Pressures. *J Bacteriol* 2009; **191**: 2574–2584.

46. Tholozan JL, Ritz M, Jugiau F, Federighi M, Tissier JP. Physiological effects of high hydrostatic pressure treatments on Listeria monocytogenes and Salmonella typhimurium. *J Appl Microbiol* 2000.

47. Molina-Gutierrez A, Stippl, VolkerDelgado A, Gänzle MG, Vogel RF, Ga MG. In Situ Determination of the Intracellular pH of Lactococcus lactis and Lactobacillus plantarum during Pressure Treatment. *Appl Environ Microbiol* 2002.

48. Molina-Höppner A, Doster W, Vogel RF, Gänzle MG. Protective Effect of Sucrose and Sodium Chloride for Lactococcus lactis during Sublethal and Lethal High-Pressure Treatments. *Appl Environ Microbiol* 2004.

621 49. Chong PLG, Fortes PAG, Jameson DM. Mechanisms of inhibition of (Na,K)-ATPase
622 by hydrostatic pressure studied with fluorescent probes. *J Biol Chem* 1985.

623 50. Smelt JPPM, Rijke AGF, Hayhurst A. Possible mechanism of high pressure
624 inactivation of microorganisms. *High Press Res* 1994; **12**: 199–203.

625 51. Mapelli F, Scoma A, Michoud G, Aulenta F, Boon N, Borin S, et al. Biotechnologies
626 for Marine Oil Spill Cleanup: Indissoluble Ties with Microorganisms. *Trends*
627 *Biotechnol* 2017; **35**: 860–870.

628 52. Dubinsky EA, Conrad ME, Chakraborty R, Bill M, Borglin SE, Hollibaugh JT, et al.
629 Succession of hydrocarbon-degrading bacteria in the aftermath of the deepwater
630 horizon oil spill in the gulf of Mexico. *Environ Sci Technol* 2013; **47**: 10860–10867.

631 53. Marietou A, Chastain R, Beulig F, Scoma A, Hazen TC, Bartlett DH. The effect of
632 hydrostatic pressure on enrichments of hydrocarbon degrading microbes from the Gulf
633 of Mexico following the deepwater Horizon oil spill. *Front Microbiol* 2018.

634 54. Yakimov MM, Giuliano L, Gentile G, Crisafi E, Chernikova TN, Abraham WR, et al.
635 Oleispira antarctica gen. nov., sp. nov., a novel hydrocarbonoclastic marine bacterium
636 isolated from Antarctic coastal sea water. *Int J Syst Evol Microbiol* 2003.

637 55. Martin DD, Bartlett DH, Roberts MF. Solute accumulation in the deep-sea bacterium
638 Photobacterium profundum. *Extremophiles* 2002; **6**: 507–514.

639 56. Simpson RK, Gilmour A. The effect of high hydrostatic pressure on the activity of
640 intracellular enzymes of Listeria monocytogenes. *Lett Appl Microbiol* 1997.

641

642 **Figures and Tables legend**

643 **Figure 1** Experimental set up. Microbial communities from hydrocarbon-free, marine

644 sediments collected at 1 000 m below sea surface level (≈10 MPa) were enriched in a HP
645 range 0.1 to 20 MPa, using either C_{20} or C_{30} as sole carbon source. Biomasses from enriched
646 consortia were characterized, including that from a third high HP reactor at 30 MPa
647 inoculated from 20 MPa reactors. Isolation from 10 and 20 MPa reactors supplied with C_{20}
648 was conducted, yielding multispecies colonies. These were pooled and tested further in a high
649 HP-adapted synthetic community (HHP-SC) at 0.1 and 10 MPa, using either C_{20} or acetate as
650 sole carbon source.

651 **Figure 2** pH decrease in enriching consortia supplied with C_{20} (**A**) or C_{30} (**B**) as sole carbon
652 source at different HPs (0.1, 10 and 20 MPa) and in two negative controls at 0.1 MPa.
653 Enriching consortia at 0.1 MPa were tested under aerobic ($+O_2$) or microaerophilic ($-O_2$)
654 conditions. Each data point represent a 10-day incubation period, after which cultures were
655 diluted 10% (v:v) and incubated again for another 10 days.

656 **Figure 3** Final cell numbers (**A** to **D**), O_2 respiration **(E**, **F**) and nutrients consumption (**G** to
657 **J**) in enriching consortia supplied with either C_{20} or C_{30} as sole carbon source at different
658 HPs (0.1, 10 and 20 MPa). Enriching consortia at 0.1 MPa were tested under aerobic ($+O_2$,
659 green) or microaerophilic ($-O_2$, yellow) conditions. In Figure **A** to **D**, cells were sorted for
660 their size using sterile filters of 25 (**A**, **B**) and 1.5 μm (**C**, **D**) prior to injection into the flow
661 cytometer for counting. Bars indicate a 95% confidence interval, with values considered
662 between the 3rd and 9th incubation (n=6). Keys: *, indicates significant difference (p <0.05)
663 with respect to 0.1 MPa $+O_2$.

664 **Figure 4** Relative 16S rRNA abundance of (**A**) bacterial families in the hydrocarbon-free,
665 marine sediment used as inoculum (original HP ≈10 MPa) and in enriching consortia, and (**B**)
666 OHCB genera detected in such enriching consortia, supplied with C_{20} (**left**) or C_{30} (**right**) as
667 sole carbon source at different HPs (0.1, 10 and 20 MPa), as assessed by Illumina
668 sequencing. Enriching consortia at 0.1 MPa were tested under aerobic ($+O_2$) or

669 microaerophilic (-O_2) conditions.

670 **Figure 5** Heatmap of the high abundant metaproteins (**top**) and radar distribution of low
671 abundant metaproteins (**bottom**) related to biological functions (UniProtKB keyword) in
672 enriching consortia supplied with C_{20} (**left**) or C_{30} (**right**) as sole carbon source at different
673 HPs (0.1, 10 and 20 MPa). Enriching consortia at 0.1 MPa were tested under aerobic (+O_2) or
674 microaerophilic (-O_2) conditions. Numbers reported in the heatmap boxes (**top**) and in the
675 radar graphs (**bottom**) represent the percentage of expressed metaprotein for a biological
676 function relative to all detected metaproteins. Complete dataset reported in Table S4; all
677 metaproteins in Table S6.

678 **Figure 6** Physiological response of HHP-SCs as compared to long-term enrichments from
679 which they derived when supplying C_{20} as sole carbon source at 0.1 and 10 MPa (n=3) (**A**,
680 pH value; **B**, cell number) and physiological response of HHP-SCs when supplied with C_{20} or
681 acetate as sole carbon source at 0.1 and 10 MPa (n=3) (**C**, final cell number; **D**, O_2 respiration
682 per cell; **E**, pH value; **F**, CO_2 production per cell). Data for enrichments is that of the last
683 three incubations (Fig. 2 and 3A,B). For convenience of comparison, HHP-SCs data when
684 supplying C_{20} is reported twice (pH, Fig. 6A and E; cell number, Fig. 6B and 6C). Bars
685 indicate the standard deviation from the mean. Keys reported in the graph.

686 **Figure 7** Mapped metaproteins involved in glycerol metabolism linked to the TCA cycle in
687 HHP-SCs supplied with C_{20} (**A**). Selected intracellular metabolites from the aqueous phase
688 (**B**) and intracellular metabolite profiles (**C**) in cells derived from HHP-SCs supplied with C_{20}
689 or acetate as sole carbon source at 0.1 (shaded area) and 10 MPa. Analyses are normalized
690 per cell content.

691 **Table 1**: High hydrostatic-pressure-adapted synthetic community (HHP-SC) composition
692 based on 16S rRNA and expression levels of proteins per each detected OTU. Reactors were

693 incubated under non-axenic conditions for 10 days, at 20°C, using either eicosane (C_{20}) or

694 acetate as sole carbon source.

Statement of authorship

AS conceived, designed and performed the experiments, and wrote the manuscript. RH performed the metaproteome analyses and co-wrote the manuscript. CD performed the metaproteome analyses. RR performed the experiments at high pressure and isolation of the micro-colonies. FMK performed the 16S rRNA analyses. IM performed the statistical analysis and the sequencing of the isolates. AM co-wrote the manuscript. PV analysed the amino acid data. HB and FM analysed the PLFA data. IMB performed surfactants analysis and general editing. KM and TV analysed intracellular compounds. DB performed the metaproteome data analysis. UR supervised the metaproteome analysis. NB funded and supervised the project. All authors reviewed the manuscripts.

Data accessibility analysis

The database for metaproteins is indicated in the Materials and Methods Section.

Enrichment

Isolation and biomass characterization

HP-adapted Synthetic Communities

Deep-sea Sample 1

+C20

Deep-sea Sample 2

+C30

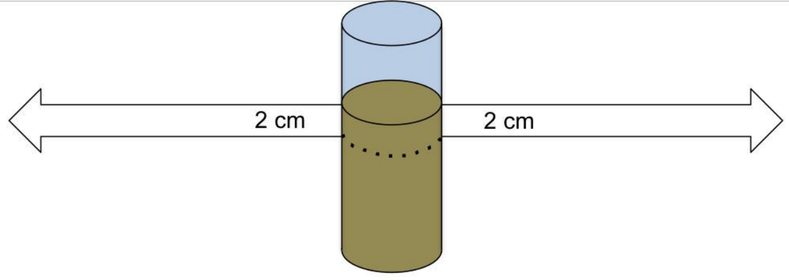

Native Depth ≈1,000 m bsl
Native HP ≈10 MPa

$-O_2$ $+O_2$

0.1 MPa | 0.1 MPa | 10 MPa | 20 MPa

10 days incubation x 9 times

0.1 MPa microaerophilic enriched biomass

0.1 MPa aerobic enriched biomass

10 MPa aerobic enriched biomass

20 MPa aerobic enriched biomass

$-O_2$ $+O_2$

0.1 MPa | 0.1 MPa | 10 MPa | 20 MPa | 30 MPa

10 days incubation x 9 times

+C20 +Acetate

$+O_2$

0.1 MPa | 10 MPa

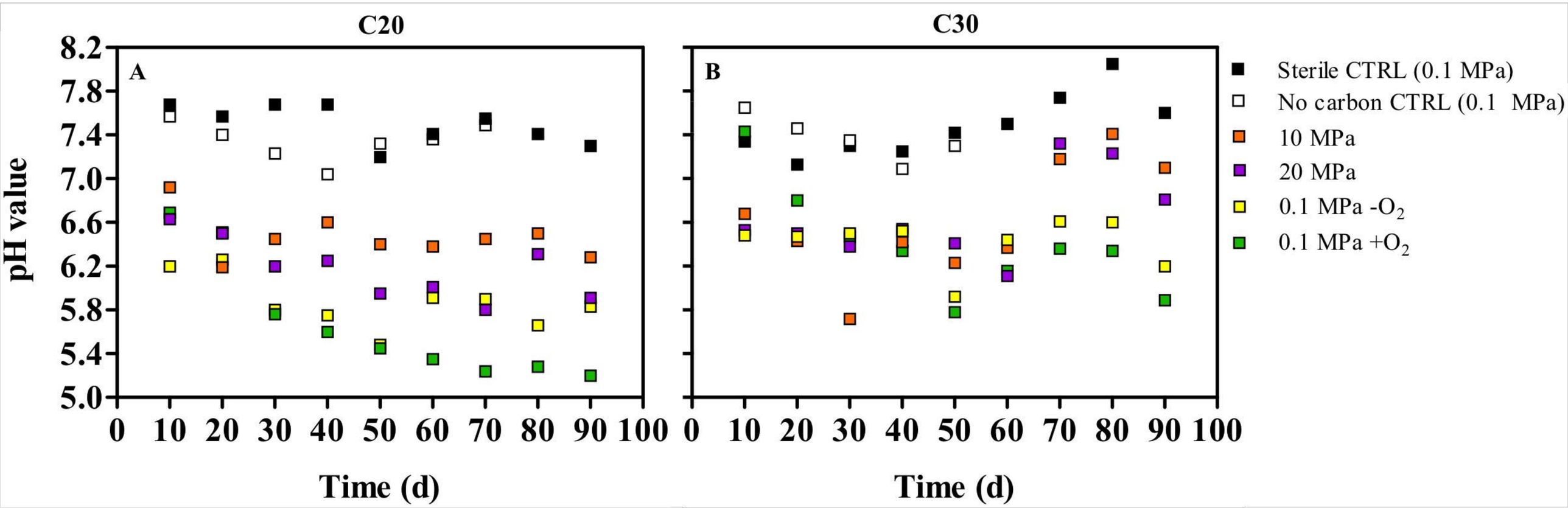
C20
C30
A
B
pH value
8.2
7.8
7.4
7.0
6.6
6.2
5.8
5.4
5.0
0
10
20
30
40
50
60
70
80
90
100
Time (d)
Sterile CTRL (0.1 MPa)
No carbon CTRL (0.1 MPa)
10 MPa
20 MPa
0.1 MPa -O2
0.1 MPa +O2

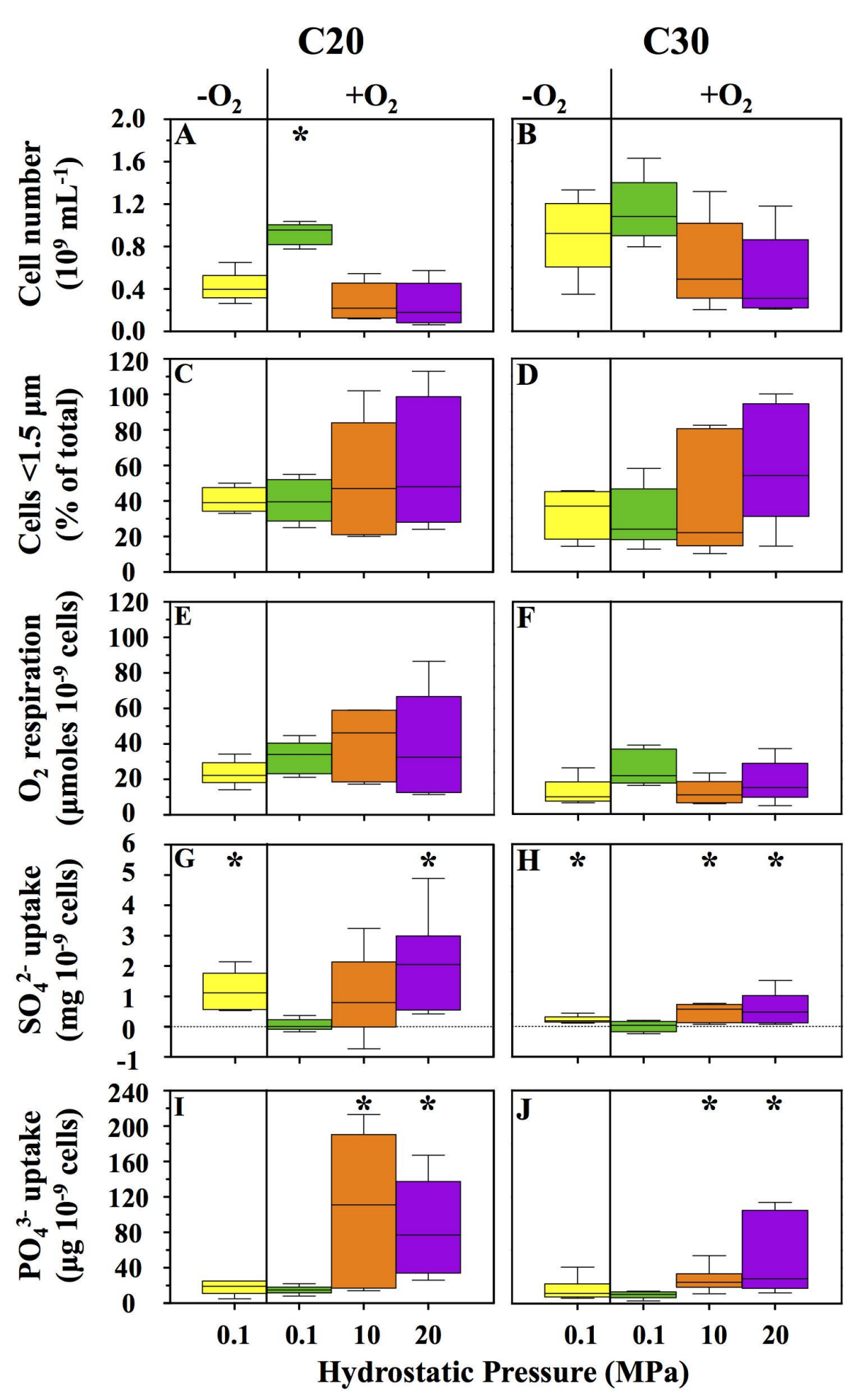
C20
C30
-O2
+O2
-O2
+O2
A
B
C
D
E
F
G
H
I
J
Cell number (10^9 mL^-1)
Cells <1.5 µm (% of total)
O2 respiration (µmoles 10^-9 cells)
SO4 2- uptake (mg 10^-9 cells)
PO4 3- uptake (µg 10^-9 cells)
0.1
0.1
10
20
0.1
0.1
10
20
Hydrostatic Pressure (MPa)

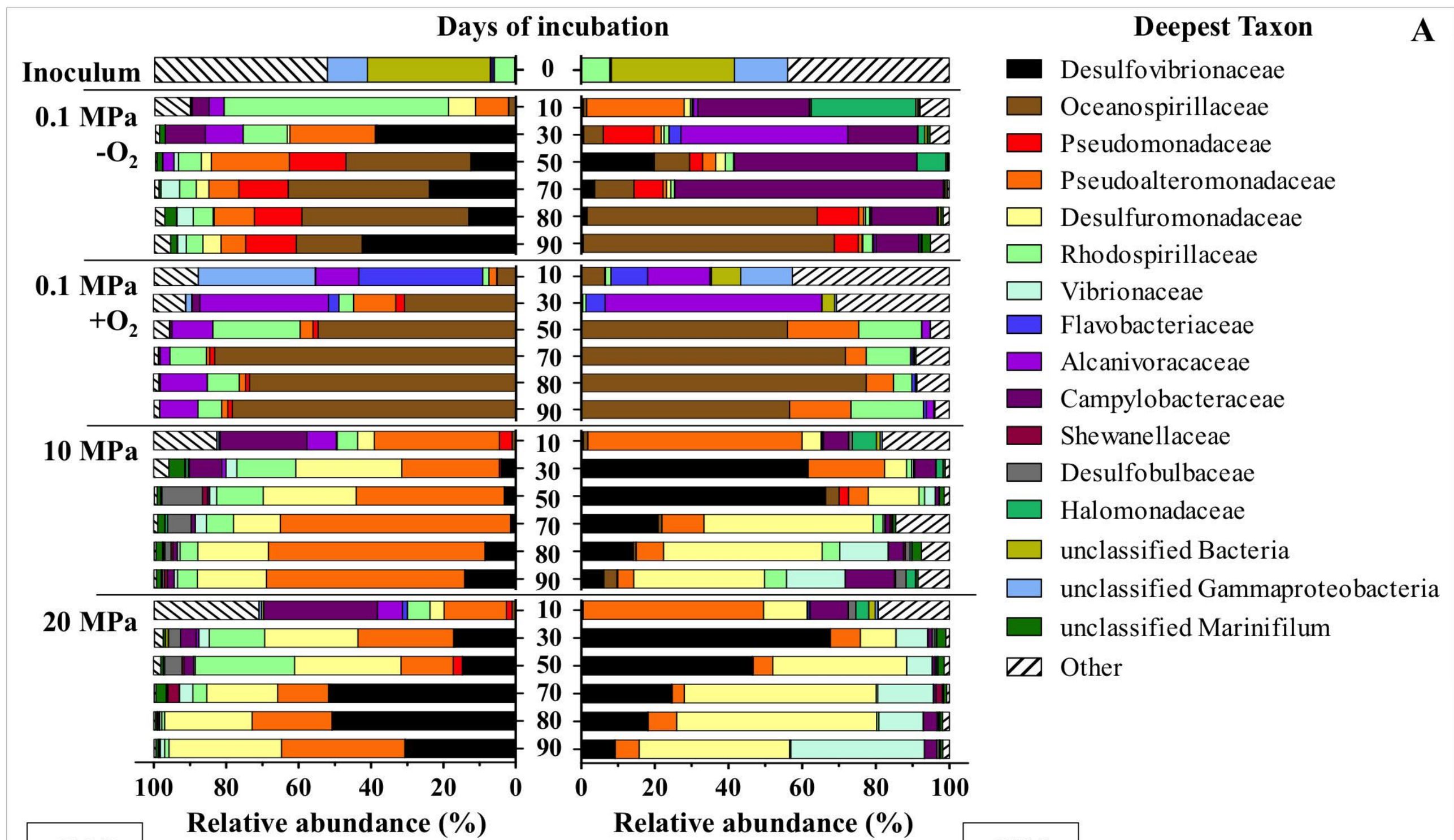
Days of incubation
Deepest Taxon
A
Inoculum
0.1 MPa -O2
0.1 MPa +O2
10 MPa
20 MPa
0
10
30
50
70
80
90
Desulfovibrionaceae
Oceanospirillaceae
Pseudomonadaceae
Pseudoalteromonadaceae
Desulfuromonadaceae
Rhodospirillaceae
Vibrionaceae
Flavobacteriaceae
Alcanivoracaceae
Campylobacteraceae
Shewanellaceae
Desulfobulbaceae
Halomonadaceae
unclassified Bacteria
unclassified Gammaproteobacteria
unclassified Marinifilum
Other
100 80 60 40 20 0
0 20 40 60 80 100
Relative abundance (%)
Relative abundance (%)

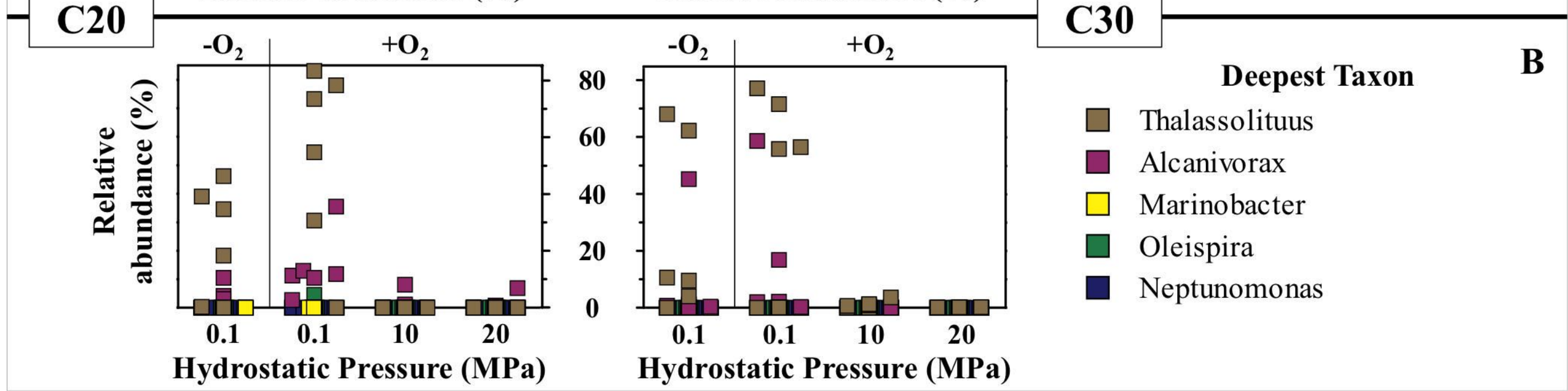
C20
C30
B
-O2
+O2
Relative abundance (%)
0
20
40
60
80
0.1
0.1
10
20
Hydrostatic Pressure (MPa)
Deepest Taxon
Thalassolituus
Alcanivorax
Marinobacter
Oleispira
Neptunomonas

Biological Function	C20					C30				
	-O_2	+O_2				-O_2	+O_2			
	0.1 MPa		10 MPa	20 MPa		0.1 MPa		10 MPa	20 MPa	
Transport	16.6	17.4	14.7	17.7	*	15.1	13.3	18.5	14.4	
Ion transport	14.4	10.8	10.3	17.0	*	10.4	8.0	15.4	14.2	**
Hydrogen ion transport	14.4	10.8	9.2	16.5	*	10.3	7.3	15.3	13.8	**
ATP synthesis	14.4	10.8	9.2	16.5	*	10.3	7.2	15.2	13.8	**
Protein biosynthesis	10.9	11.2	13.3	11.5		8.3	11.0	12.7	12.6	
Tricarboxylic acid cycle	4.7	5.3	8.6	3.6	*	4.5	4.4	5.2	2.6	*
Amino-acid biosynthesis	2.7	4.0	4.9	2.1	*	4.5	4.1	2.5	3.9	
Glycolysis	1.0	0.8	0.6	0.6		1.6	2.1	2.2	4.6	*
Transcription	3.9	4.0	4.0	1.8	*	4.0	9.0	1.0	1.2	**
One-carbon metabolism	1.1	2.8	0.5	0.4	**	2.9	3.3	0.5	0.6	**

Legend

** 0.1 MPa *vs.* ≥ 10 MPa
* 0.1 MPa *vs.* 20 MPa

0.1 MPa -O_2
0.1 MPa +O_2
10 MPa
20 MPa

High abundant proteins

Low abundant proteins

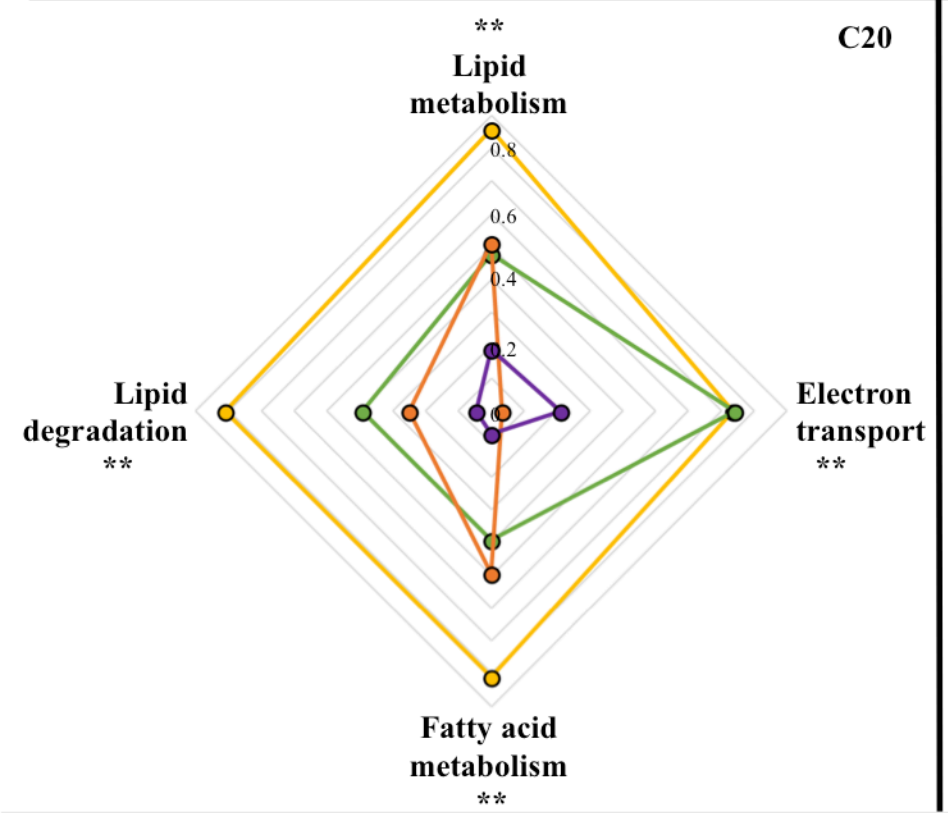

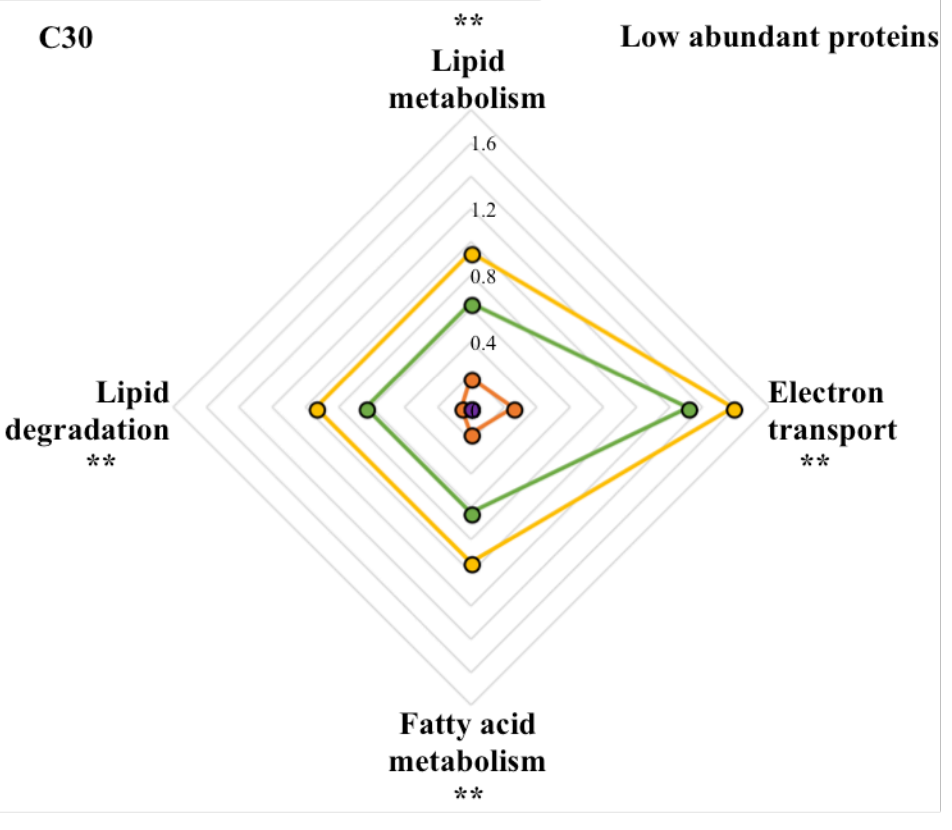

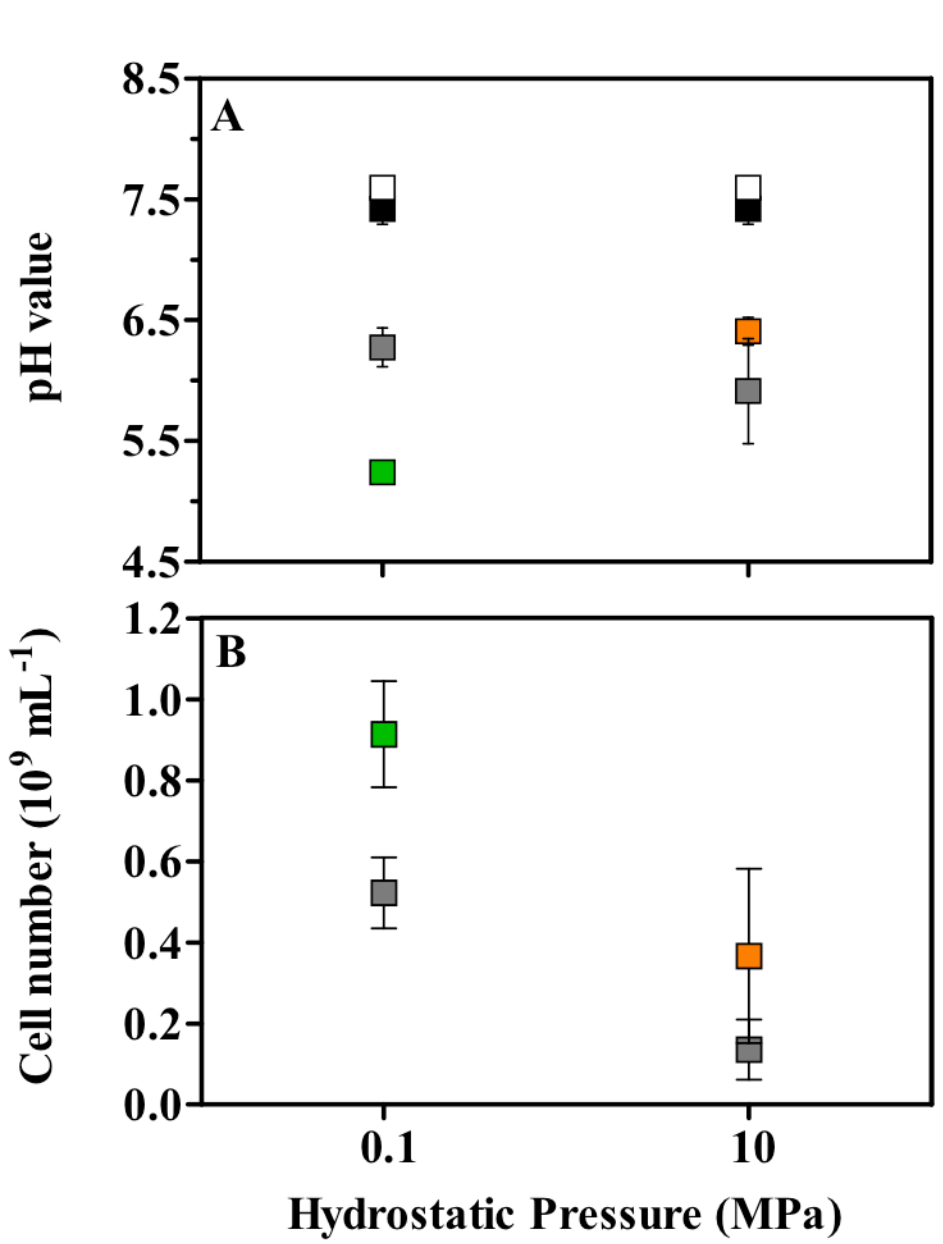

CTRL Enriched consortia

CTRL Synthetic communities

Enriched consortia at 0.1 MPa

Enriched consortia at 10 MPa

Hydrostatic-pressure-adapted Synthetic communities (HHP-SCs)

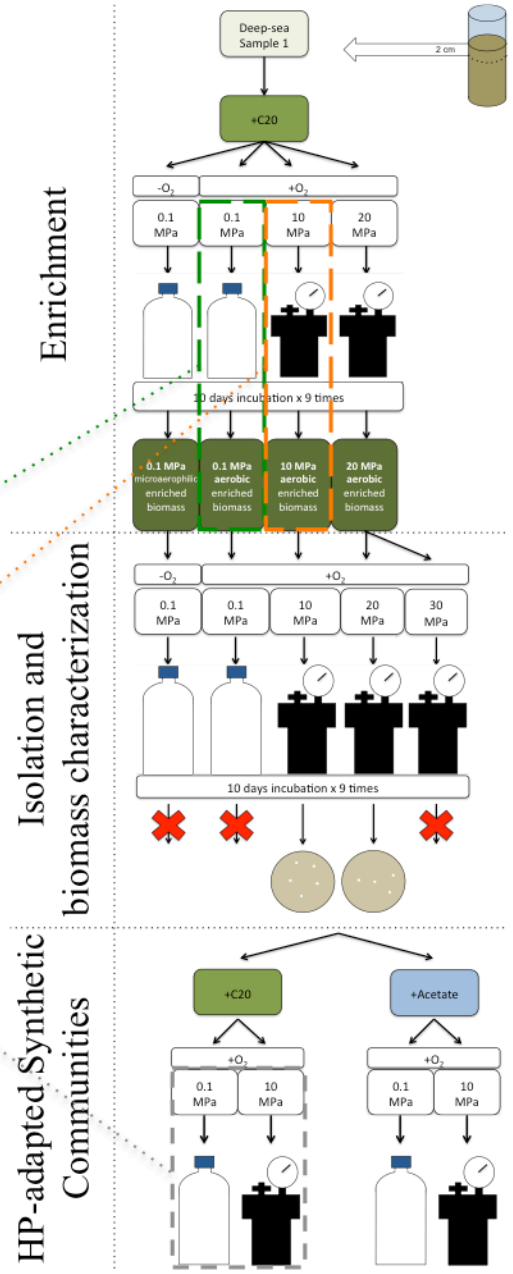

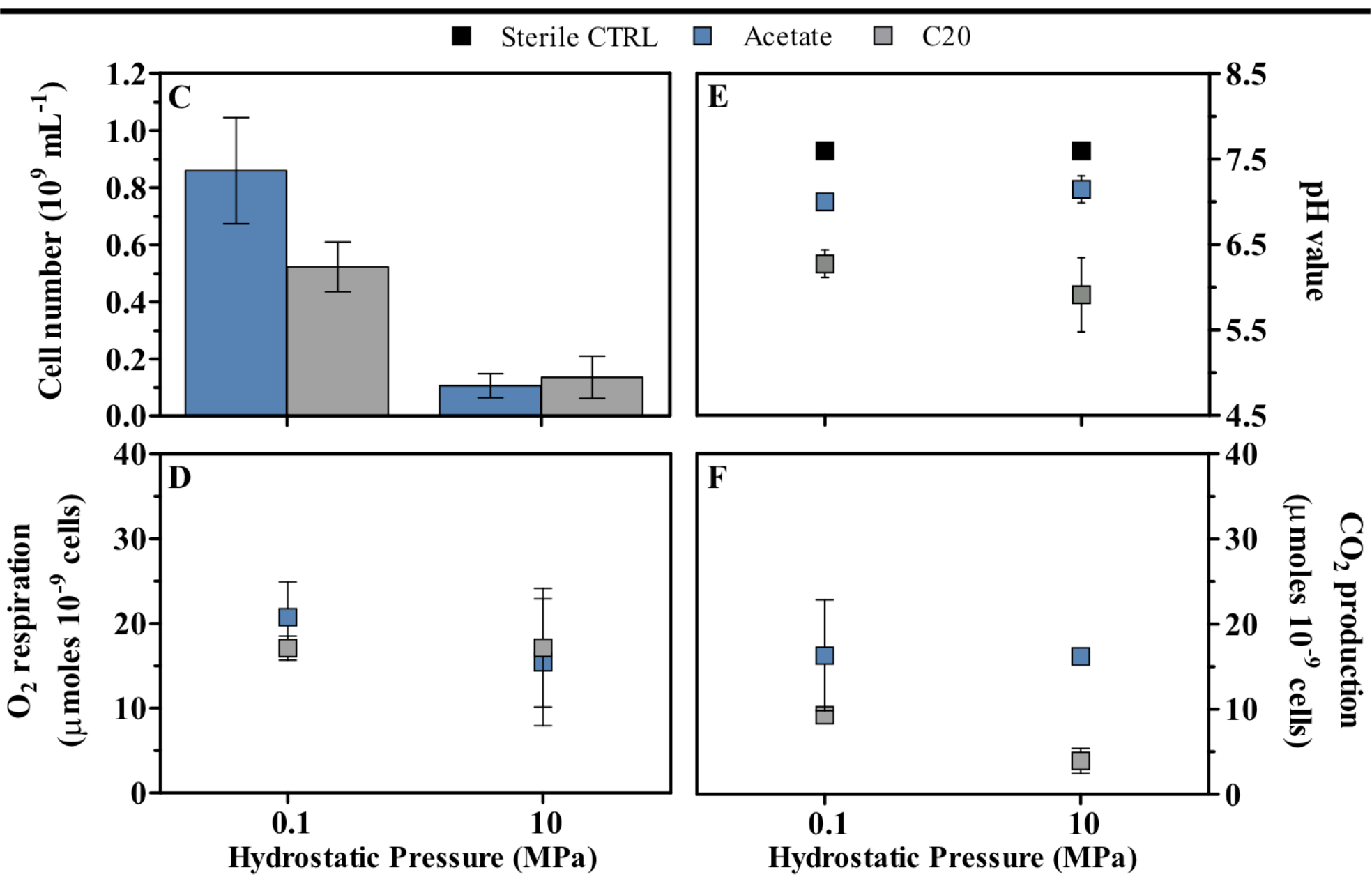

A

Fructose 1,6 bisphosphate

Name	Fructose-bisphosphate aldolase
EC	4.1.2.13
Taxonomy	Vibrio, Thalassospira, Gammaproteobacteria

Glyceraldehyde 3-phosphate

Name	Glyceraldehyde-3-phosphate dehydrogenase
EC	1.2.1.-
Taxonomy	Vibrio, Thalassospira, Pseudomonas

NAD^+ / NADH

1,3-Biphosphoglycerate

Name	Triose-phosphate isomerase
EC	5.3.1.1
Taxonomy	Halomonas, Vibrio, Thalassospira

ADP / ATP

Name	Phosphoglycerate kinase
EC	2.7.2.3
Taxonomy	Vibrio, Thalassospira

Dihydroxyacetone-Phosphate

3-Phosphoglycerate

Name	Dihydroxyacetone kinase
EC	2.7.1.29
Taxonomy	Vibrio, Thalassospira

Name	Glycerol-3-phosphate dehydrogenase
EC	1.1.5.3
Taxonomy	Vibrio

Name	Glycerol-3-phosphate dehydrogenase [NAD(P)+]
EC	1.1.1.94
Taxonomy	Pseudoalteromonas, Pseudomonas

Name	Phosphoglycerate mutase
EC	5.4.2.12
Taxonomy	Vibrio, Thalassospira

ADP / ATP

Glycerol-3 Phosphate

NAD^+ / $NAD(P)^+$

NADH / NADPH

2-Phosphoglycerate

Dihydroxyacetone

Name	Glycerol Kinase
EC	2.7.1.30
Taxonomy	Vibrio,Thalassospira

Name	Enolase
EC	4.2.1.11
Taxonomy	Vibrio, Thalassospira, Halomonas, Pseudoaltermonas

ADP / ATP

Glycerol

Phosphoenolpyruvate

Pyruvate

Name	Phosphoenolpyruvate synthase
EC	2.7.9.2
Taxonomy	Vibrio, Halomonas

ADP / ATP

Name	Phosphoenolpyruvate carboxykinase
EC	4.1.1.49
Taxonomy	Vibrio, Thalassospira

Oxaloacetate

Citrate

Name	Citrate synthase
EC	2.3.3.1
Taxonomy	Vibrio, Thalassolituus, Pseudoalteromonas, Microbacterium, Halomonas

Glycerol metabolism

Glycolysis

TCA Cycle

B

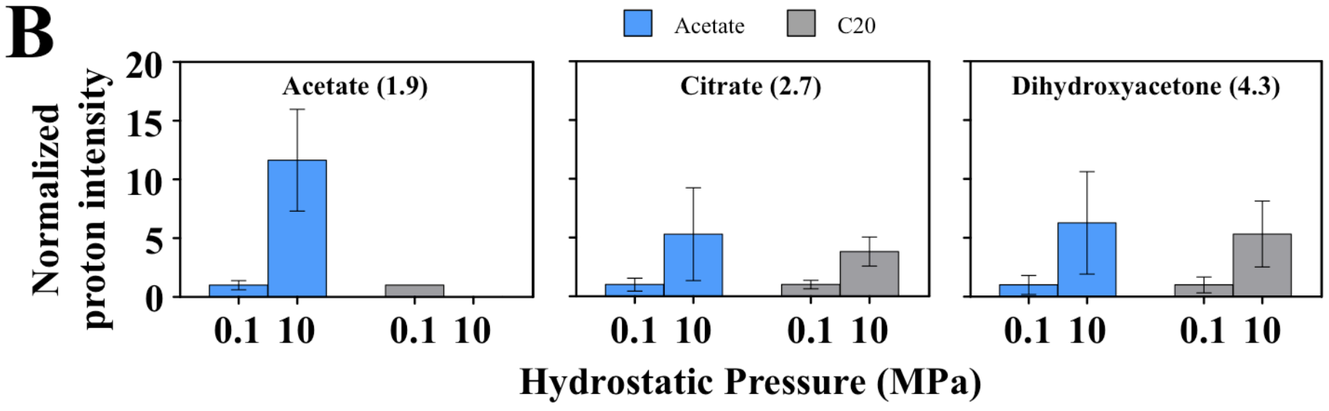

C

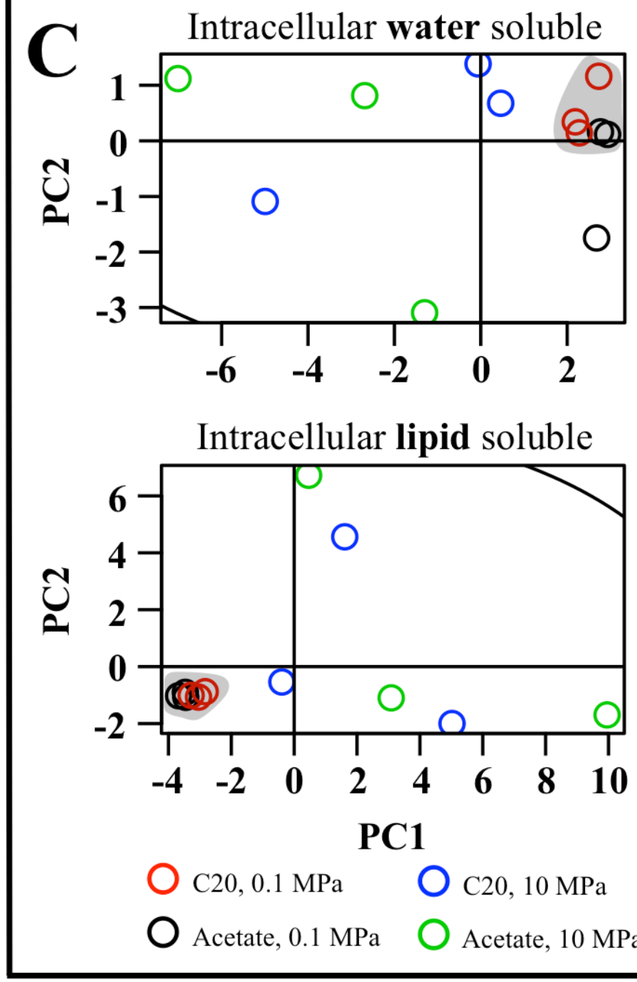

Table 1: High hydrostatic-pressure-adapted synthetic community (HHP-SC) composition based on 16S rRNA and expression levels of proteins per each detected OTU. Reactors were incubated under non-axenic conditions for 10 days, at 20 °C, using either eicosane (C_{20}) or acetate as sole carbon source.

Main members of the HHP-SC	OTU	Taxonomy	16S rRNA									Metaproteins								
			Acetate					C_{20}				Acetate					C_{20}			
			0.1 MPa		10 MPa		10 *vs.* 0.1 MPa	0.1 MPa		10 MPa		10 *vs.* 0.1 MPa	0.1 MPa		10 MPa		10 *vs.* 0.1 MPa	0.1 MPa		10 MPa		10 *vs.* 0.1 MPa
			Mean	s.d.	Mean	s.d.	log2 fold change	Mean	s.d.	Mean	s.d.	log2 fold change	Mean	s.d.	Mean	s.d.	log2 fold change	Mean	s.d.	Mean	s.d.	log2 fold change
Core	Otu00001	*Vibrio*	70.9	3.0	17.2	2.2	-2.05	65.7	3.3	60.2	21.7	-0.13	51.5	0.7	50.7	3.3	-0.02	50.5	0.7	44.9	3.3	-0.17
	Otu00002	*Thalassospira*	16.7	1.7	34.8	10.6	1.06	9.2	1.4	21.6	10.8	1.24	23.0	0.3	22.1	2.9	-0.06	21.5	1.5	24.5	2.7	0.19
	Otu00003	*Halomonas*	4.2	1.1	37.1	5.7	3.15	2.7	0.4	11.2	6.7	2.06	7.9	0.3	9.1	0.3	0.20	8.2	0.3	7.9	0.6	-0.05
	Otu00004	*Pseudoalteromonas*	1.0	0.2	1.9	1.0	0.92	9.6	2.5	3.4	3.1	-1.52	7.0	0.7	6.2	0.6	-0.18	6.5	1.1	8.8	0.4	0.44
Satellite	Otu00005	*Thalassolituus*	0.0	0.0	0.1	0.0	3.97	10.7	1.4	1.5	1.0	-2.79	0.0	0.0	0.0	0.0	-	2.9	0.0	5.9	0.0	1.02
	Otu00006	*Pseudomonas*	6.4	1.3	7.7	2.6	0.27	0.7	0.4	0.3	0.4	-1.09	5.6	0.2	6.2	0.2	0.15	7.6	1.2	4.2	0.4	-0.86
	Otu00007	*Microbacterium*	0.0	0.0	0.0	0.0	-	0.4	0.2	1.2	0.4	1.60	0.1	0.0	0.1	0.1	-	0.1	0.1	0.2	0.1	1.00
	Otu00008	*Clostridium*	0.0	0.0	0.7	1.1	-	0.0	0.0	0.0	0.0	-	0.0	0.0	0.0	0.0	-	0.0	0.0	0.0	0.0	-
Core community (% of total)			92.8		91.0			87.2		96.4			89.4		88.1			86.7		86.1		
Main 8 OTUs (% of total)			99.2		99.4			99.0		99.4			95.1		94.4			97.3		96.4		